

Article

# Application of the Bland–Altman and Receiver Operating Characteristic (ROC) Approaches to Study Isotope Effects in Gas Chromatography–Mass Spectrometry Analysis of Human Plasma, Serum and Urine Samples

Dimitrios Tsikas 

Core Unit Proteomics, Institute of Toxicology, Hannover Medical School, 30623 Hannover, Germany; tsikas.dimitros@mh-hannover.de

**Abstract:** The Bland–Altman approach is one of the most widely used mathematical approaches for method comparison and analytical agreement. This work describes, for the first time, the application of Bland–Altman to study  $^{14}\text{N}/^{15}\text{N}$  and  $^1\text{H}/^2\text{H}$  (D) chromatographic isotope effects of endogenous analytes of the L-arginine/nitric oxide pathway in human plasma, serum and urine samples in GC-MS. The investigated analytes included arginine, asymmetric dimethylarginine, dimethylamine, nitrite, nitrate and creatinine. There was a close correlation between the percentage difference of the retention times of the isotopologs of the Bland–Altman approach and the area under the curve (AUC) values of the receiver operating characteristic (ROC) approach ( $r = 0.8619$ ,  $p = 0.0047$ ). The results of the study suggest that the chromatographic isotope effects in GC-MS result from differences in the interaction strengths of H/D isotopes in the derivatives with the hydrophobic stationary phase of the GC column. D atoms attenuate the interaction of the skeleton of the molecules with the lipophilic GC stationary phase. Differences in isotope effects in plasma or serum and urine in GC-MS are suggested to be due to a kind of matrix effect, and this remains to be investigated in forthcoming studies using Bland–Altman and ROC approaches.

**Keywords:** Bland–Altman; chromatography; isotope effects; GC-MS; retention time; ROC



**Citation:** Tsikas, D. Application of the Bland–Altman and Receiver Operating Characteristic (ROC) Approaches to Study Isotope Effects in Gas Chromatography–Mass Spectrometry Analysis of Human Plasma, Serum and Urine Samples. *Molecules* **2024**, *29*, 365. <https://doi.org/10.3390/molecules29020365>

Academic Editors: Victoria Samanidou and Paraskevas D. Tzanavaras

Received: 12 December 2023  
Revised: 8 January 2024  
Accepted: 9 January 2024  
Published: 11 January 2024



**Copyright:** © 2024 by the author. Licensee MDPI, Basel, Switzerland. This article is an open access article distributed under the terms and conditions of the Creative Commons Attribution (CC BY) license (<https://creativecommons.org/licenses/by/4.0/>).

## 1. Introduction

In gas chromatography (GC) and reversed-phase liquid chromatography (LC), isotopologs differ in their retention times, with deuterated compounds having, as a rule, smaller retention times ( $t_R$ ) than their protiated analogs [1]. The slightly reduced molecular volume of  $^2\text{H}$ -labeled compounds compared to their non-labeled analogs is assumed to be responsible for this phenomenon [2]. The  $t_R$  of the isotopologs is the main parameter for quantitate H/D isotope effects [3]. One method to calculate the H/D isotope effect (IE) is to divide the  $t_R$  of the protiated analyte  $t_{R(H)}$  by the  $t_R$  of the deuterated analyte  $t_{R(D)}$  (Formula (1)). The difference in the retention times can be used to estimate the extent of the isotope effect  $\delta_{(H/D)}$  (Formula (2)). The closer the IE value to the unity (1.0000), the lower/weaker the isotope effect between the isotopologs. The smaller the difference  $\delta_{(H/D)}$  in the retention times  $t_{R(H)}$  and  $t_{R(D)}$ , the higher/stronger the isotope effect between the isotopologs. These issues are also valid for isotopes of other elements, including  $^{14}\text{N}$  and  $^{15}\text{N}$ .

$$\text{IE} = t_{R(H)} / t_{R(D)} \quad (1)$$

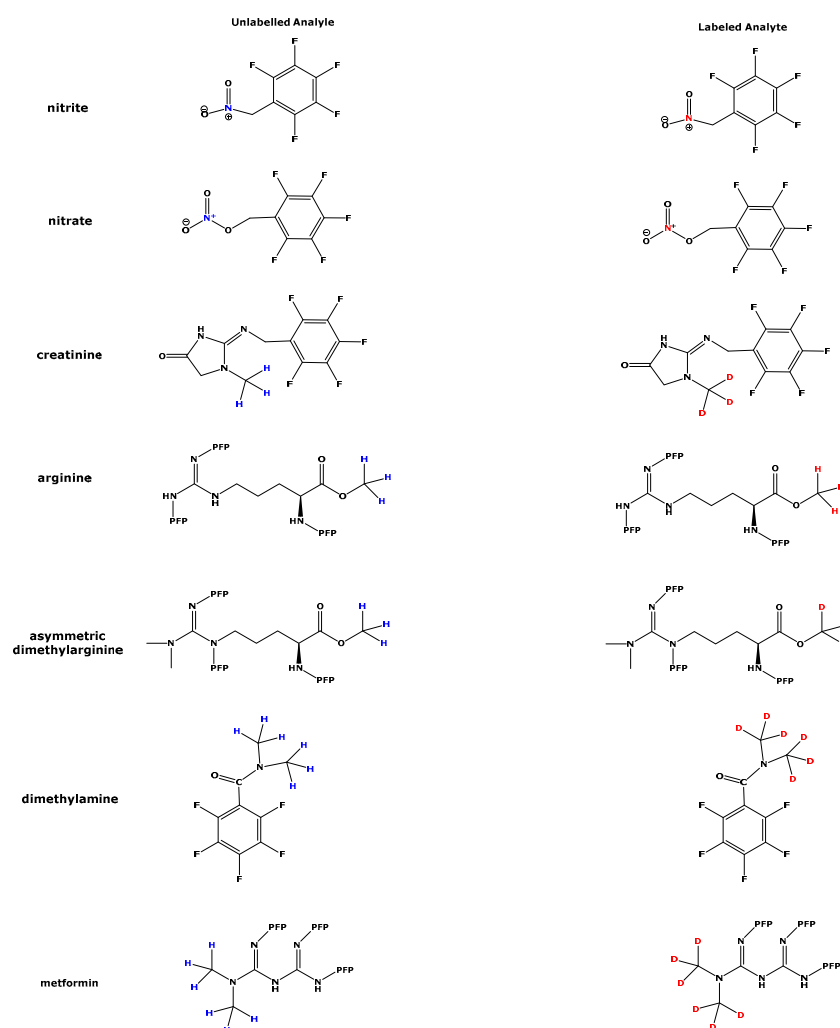
$$\delta_{(H/D)} = t_{R(H)} - t_{R(D)} \quad (2)$$

$$\mu_{(H/D)} = 1/2 \times (t_{R(H)} + t_{R(D)}) \quad (3)$$

$$\delta (\%) = 2 \times ((t_{R(H)} - t_{R(D)})/[t_{R(H)} + t_{R(D)}]) \times 100 \quad (4)$$

The Bland–Altman approach is useful for the comparison of methods with comparable analytical performance [4,5]. It is a graphical approach which examines the relationship between the difference ( $\delta$ ) of the values obtained by two methods and the average ( $\mu$ ) of the methods. In a variant of the Bland–Altman method, the percentage difference  $\delta$  (%) of the two methods is plotted versus the average of these methods (Formulas (3) and (4)). One may expect that the Bland–Altman approach would be useful in calculating the absolute and percentage difference of the retention times of isotopologs as measures of isotope effects. The Bland–Altman method has been sporadically used in this area, including  $\delta(^{18}\text{O})$  isotope ratios [6–8]. The receiver operating characteristic (ROC) approach is another graphical plot that is widely used in several disciplines, notably including clinical chemistry [9,10]. The utility of the ROC approach in comparison to methods in analytical chemistry has been demonstrated [5]. The ROC approach is useful for evaluating the agreement/disagreement between the isotopologs.

In the present work, the Bland–Altman and ROC approaches were used for the first time to investigate the H/D and  $^{14}\text{N}/^{15}\text{N}$  isotope effects of endogenous substances in human plasma, serum and urine samples. The analytes considered in the study belong to the L-arginine/nitric oxide pathway [11]. They include nitrite and nitrate, the major metabolites of nitric oxide (NO), L-arginine (Arg) and asymmetric dimethylarginine (ADMA), the endogenous substrate and inhibitor of NO synthase, respectively [11], and dimethylamine (DMA), the major urinary metabolite of ADMA [12]. In addition, creatinine serves as an analyte that is commonly used to correct for the excretion of endogenous substances in urine collected by spontaneous micturition. The above-mentioned analytes were measured by gas chromatography–mass spectrometry (GC-MS) after proper chemical derivatization. The chemical structures of the derivatives of the protiated (unlabeled) and  $^2\text{H}$ - or  $^{15}\text{N}$ -labelled analytes are shown in Scheme 1.



**Scheme 1.** Chemical structures of the unlabeled analytes (**left**) and their  $^{15}\text{N}$  and  $^2\text{H}$  (D) isotopologs (**right**) investigated in the present work. Nitrite, nitrite and creatinine were derivatized with pentafluorobenzyl bromide in aqueous acetone (e.g., 60 min at 50 °C). Arginine and asymmetric dimethylarginine were first methylated in 2 M HCl in  $\text{CH}_3\text{OH}$  or 2 M HCl in  $\text{CD}_3\text{OD}$  (e.g., 30 min at 80 °C) and then acylated by pentafluoropropionic anhydride in ethyl acetate (e.g., 60 min at 65 °C). Metformin was derivatized with pentafluoropropionic anhydride only. Dimethylamine was derivatized with pentafluorobenzoyl chloride at room temperature. PFB, pentafluorobenzyl; PFP, pentafluoropropionyl. Blue color indicates  $^{14}\text{N}$  and  $^1\text{H}$  isotopes; red color indicates  $^{15}\text{N}$  and  $^2\text{H}$  (D) isotopes.

## 2. Methods

### 2.1. GC-MS Analyses in Human Plasma, Serum and Urine Samples

The human plasma, serum and urine samples analyzed in the present work were collected in previous clinical studies of the author's group and cooperating groups after approval by the local ethics committees [13–19]. The studies were conducted in line with the ethical principles of the Declaration of Helsinki [20]. The COVID-19 study [17] was approved by the local ethics committees (9948\_BO\_K\_2021 Hannover Medical School; 29/3/21 University Medical Center Göttingen). The ASOS study was approved by the Health Research Ethics Committee of North-West University (NWU-00007-15-A1) [18].

Nitrite and nitrate were analyzed simultaneously by GC-MS as described previously, using commercially available  $^{15}\text{N}$ -nitrite and  $^{15}\text{N}$ -nitrate as internal standards, respectively [13]. Creatinine was analyzed via GC-MS as described elsewhere using commercially available [*methyl*- $^2\text{H}_3$ ] creatinine as internal standard [14]. Arg and ADMA were analyzed by GC-MS, using in situ prepared trideuteromethyl ester as described previously [15]. DMA

was analyzed by GC-MS using [*dimethyl*- $^2\text{H}_3$ ]DMA ( $d_6$ -DMA) as the internal standard [16]. Metformin (METF) was analyzed by GC-MS using [*dimethyl*- $^2\text{H}_3$ ]metformin ( $d_6$ -METF) as the internal standard [19]. The isotopic purity in the stable-isotope-labeled analogs was at least 99% at  $^2\text{H}$  and  $^{15}\text{N}$ . The concentrations of the internal standards were 1  $\mu\text{M}$  for ADMA in plasma and serum; 20  $\mu\text{M}$  in urine; 50  $\mu\text{M}$  for Arg in plasma and serum; 10 mM and 1 mM for creatinine in urine and serum, respectively; 1 mM for DMA in urine; 4  $\mu\text{M}$  for nitrite in plasma and serum and 8  $\mu\text{M}$  in urine; 40  $\mu\text{M}$  for nitrate in plasma and 800  $\mu\text{M}$  in urine.

GC-MS analyses were performed on the apparatus model ISQ from ThermoFisher (Dreieich, Germany), which was equipped with a fused silica capillary OPTIMA-17 column (15 m  $\times$  0.25 mm, 0.25  $\mu\text{m}$  film thickness) from Macherey-Nagel (Düren, Germany). Helium and methane were, respectively, used as carrier and reagent gases for negative-ion chemical ionization. Analyses were performed by selected-ion monitoring (SIM) for nitrite, nitrate, creatinine, DMA, ADMA and Arg. Aliquots of 1  $\mu\text{L}$  toluene (for amino acids, DMA and metformin) or ethyl acetate (for nitrite, nitrate and creatinine) extracts of the derivatives were injected in the splitless mode. Ions were detected after conversion to electrons by using an electron multiplier. Different oven temperature programs were used, starting either at 40  $^\circ\text{C}$  or 70  $^\circ\text{C}$  (for nitrite, nitrate and creatinine).

## 2.2. Calculations

Isotope effect values were calculated using Formula (1). The difference (in min) between the retention times was calculated by Formula (2). The difference in the retention times was multiplied by 60 to obtain the outcome in seconds. In the Bland–Altman approach, the percentage difference ( $\delta$  (%)) was plotted versus the average ( $\mu_{(H/D)}$ ). The term bias (%) in the regular Bland–Altman approach corresponds to  $\delta$  (%). The receiver operating characteristic (ROC) approach was used to determine the area under the curve (AUC) values by using the retention times of the isotopologs. The ratios of the peak areas (PAR) of endogenous analytes and the respective internal standards were calculated and used to test for potential correlations between the difference  $\delta$  and the PAR values. The Wilcoxon matched-pairs signed-rank test was used to test statistical differences in the retention times of isotopologs.

## 2.3. Statistical Analyses and Data Presentation

GraphPad Prism Version 7 for Windows (GraphPad Software, San Diego, CA, USA) was used for statistical analyses and preparation of graphs, including the Bland–Altman and ROC plots. The ROC approach was used to calculate AUC values and evaluate agreement/disagreement between the isotopologs. AUC values are reported as mean with standard error. The Wilcoxon matched-pairs signed-rank test was used in two-tailed paired analyses. A  $p$ -value of  $<0.05$  was considered significant. Chemical structures of the investigated derivatives of the isotopologs were drawn using ChemDraw 15.0 Professional (PerkinElmer, Germany).

## 3. Results

### 3.1. Bland–Altman and ROC Approaches to Study Isotope Effects in GC-MS in Biological Samples

The primary results of the present study are listed in Table 1. The secondary results obtained from the application of the Bland–Altman and ROC approaches are summarized in Table 2 and shown in Figure 1.

The retention times of all derivatives were measured with high precision (Table 1). The  $^2\text{H}$  and  $^{15}\text{N}$  isotopologs had smaller retention times than their  $^1\text{H}$  and  $^{14}\text{N}$  counterparts. Yet, the differences in the retention times were larger for the  $^2\text{H}$  analogs. The IE values for the  $^{15}\text{N}$  derivatives of nitrite and nitrate in plasma and urine were practically 1.0000, and the difference in the retention times was not higher than 0.18 s. The highest IE and  $\delta$  values were observed for the PFBz derivative of  $d_6$ -DMA, i.e., 1.007 and 1.5 s, respectively. The concentrations of the stable-isotope labeled analogs, which were added to the plasma and

urine samples, were all relevant for the respective biological samples. This is indicated by the measured PAR values for all analytes, which ranged between 0.2 and 2.4. Weak correlations after Spearman between the PAR and  $\delta$  values were observed for some analytes, indicating a very weak dependence of  $\delta$  upon the endogenous analyte concentrations in the plasma and urine samples analyzed.

**Table 1.** Summary of the results of the GC-MS (ISQ) analyses of the investigated analytes in human plasma and urine samples in the present work. The coefficients of variation are reported in parentheses. Me, methyl; PAR, peak area ratio; PFB, pentafluorobenzyl; PFBz, pentafluorobenzoyl; PFP, pentafluoropropionyl; P, plasma; U, urine. The dwell time was 50 ms or 100 ms. The Wilcoxon test  $p$ -values were <0.0001. See also: Scheme 1.

Analyte	Derivative	$m/z$	Retention Time (min)	IE	$\Delta$ (s)	PAR	Spearman PAR vs. $\delta$
$^{14}\text{N}$ -Nitrite-U	PFB	46	4.517 (0.05)	1.00000	0.07839	0.227 $\pm$ 0.232	none
$^{15}\text{N}$ -Nitrite-U	PFB	47	4.516 (0.00)	(0.05)	(115)		
$^{14}\text{N}$ -Nitrate-U	PFB	62	4.325 (0.02)	1.00000	0.10450	0.947 $\pm$ 0.575	$r = 0.265$
$^{15}\text{N}$ -Nitrate-U	PFB	63	4.323 (0.05)	(0.05)	(165)		$p = 0.037$
$^{14}\text{N}$ -Nitrite-P	PFB	46	4.521 (0.02)	1.00000	0.0228	0.234 $\pm$ 0.175	$r = 0.217$
$^{15}\text{N}$ -Nitrite-P	PFB	47	4.520 (0.03)	(0.03)	(342)		$p = 0.030$
$^{14}\text{N}$ -Nitrate-P	PFB	62	4.328 (0.06)	1.00100	0.1794	0.69 $\pm$ 0.42	none
$^{15}\text{N}$ -Nitrate-P	PFB	63	4.325 (0.01)	(0.06)	(82)		
$^1\text{H}$ -Creatinine-U	PFB	112	6.913 (0.02)	1.00100	0.6022	0.602 $\pm$ 0.081	$r = 0.316$
$^2\text{H}_3$ -Creatinine-U	PFB	115	6.903 (0.01)	(0.02)	(13)		$p = 0.019$
$^1\text{H}$ -Arg-P	$d_0\text{Me-PFP}$	586	5.729 (0.05)	1.00200	0.699	2.14 $\pm$ 1.27	none
$^2\text{H}_3$ -Arg-P	$d_3\text{Me-PFP}$	589	5.718 (0.05)	(0.03)	(13)		
$^1\text{H}$ -ADMA-P	$d_0\text{Me-PFP}$	634 $\rightarrow$ 378	10.85 (0.02)	1.00100	0.9168	0.493 $\pm$ 0.96	none
$^2\text{H}_3$ -ADMA-P	$d_3\text{Me-PFP}$	637 $\rightarrow$ 378	10.84 (0.02)	(0.02)	(12)		
$^1\text{H}$ -ADMA-U	$d_0\text{Me-PFP}$	634 $\rightarrow$ 378	10.97 (0.09)	1.00100	0.8538	2.35 $\pm$ 1.26	none
$^2\text{H}_3$ -ADMA-U	$d_3\text{Me-PFP}$	637 $\rightarrow$ 378	10.95 (0.09)	(0.02)	(13)		
$^1\text{H}$ -DMA-U	PFBz	240	3.520 (0.17)	1.007	1.502	0.436 $\pm$ 0.348	$r = -0.183$
$^2\text{H}_6$ -DMA-U	PFBz	246	3.495 (0.17)	(0.14)	(20)		$p = 0.041$

**Table 2.** Summary of the results of the GC-MS (ISQ) analyses of the investigated analytes in human plasma and urine samples in the present work as obtained by the (A) Bland–Altman and (B) AUC-ROC approaches. P, plasma; U, urine; LOA, limit of agreement; SD, standard deviation; SE, standard error.

Analyte	(A) Bland–Altman			(B) ROC	
	$\delta$ (%)	SD (%)	95% Lowest LOA	95% Highest LOA	AUC (Mean $\pm$ SE)
DMA-U ( $n = 62$ )	0.714	0.143	0.4333	0.9946	0.9951 $\pm$ 0.0024 $p < 0.0001$
Arginine-P ( $n = 100$ )	0.2035	0.02725	0.1501	0.2570	0.9932 $\pm$ 0.0054 $p < 0.0001$

Table 2. Cont.

Analyte	(A) Bland–Altman				(B) ROC
	$\delta$ (%)	SD (%)	95% Lowest LOA	95% Highest LOA	AUC (Mean $\pm$ SE)
Creatinine-U ( <i>n</i> = 55)	0.1453	0.01949	0.1071	0.1835	1.000 $\pm$ 0.000 <i>p</i> < 0.0001
ADMA-P ( <i>n</i> = 50)	0.1409	0.01698	0.1076	0.1742	1.000 $\pm$ 0.000 <i>p</i> < 0.0001
ADMA-U ( <i>n</i> = 52)	0.1298	0.01630	0.0979	0.1618	0.8299 $\pm$ 0.0384 <i>p</i> < 0.0001
Nitrate-P ( <i>n</i> = 100)	0.06909	0.05674	−0.0421	0.1803	0.7951 $\pm$ 0.033 <i>p</i> < 0.0001
Nitrate-U ( <i>n</i> = 62)	0.04029	0.04625	−0.0504	0.1309	0.7177 $\pm$ 0.0469 <i>p</i> < 0.0001
Nitrite-U ( <i>n</i> = 52)	0.02891	0.04768	−0.0646	0.1224	0.6371 $\pm$ 0.050 <i>p</i> = 0.008
Nitrite-P ( <i>n</i> = 100)	0.00841	0.02879	−0.0480	0.0648	0.5414 $\pm$ 0.041 <i>p</i> = 0.311

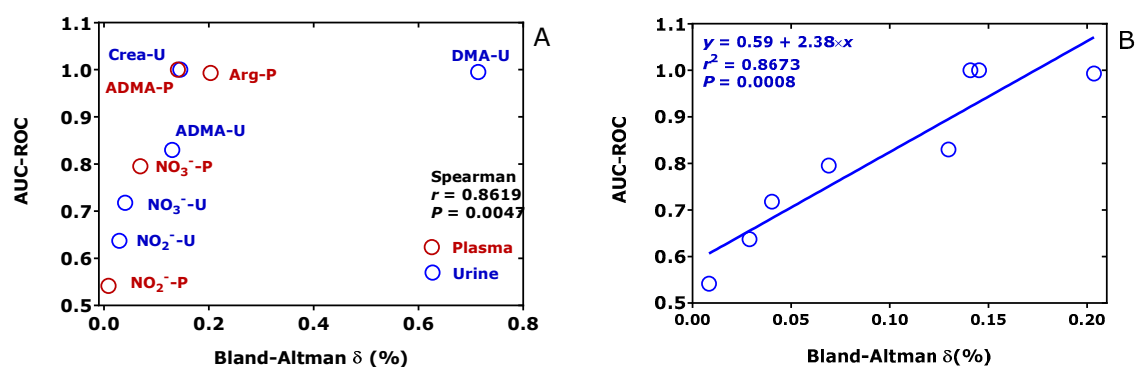


**Figure 1.** Comparison of the ROC and Bland–Altman approaches. (A) The mean AUC-ROC values are plotted versus the percentage differences  $\delta$  (%) of the retention times of the isotopologs of the indicated analytes in plasma (P) and urine (U). There is a close correlation after Spearman among the two approaches. (B) The mean AUC-ROC values are plotted versus the percentage differences  $\delta$  (%) in the retention times of the isotopologs of the investigated analytes in plasma and urine; the value of DMA was not considered.

The application of the Bland–Altman approach resulted in  $\delta$  (%) values ranging between 0.714% for DMA in urine and 0.00841% for the PFB derivative of nitrite in plasma (Table 2). The application of the ROC approach resulted in AUC values ranging between 1.0000 for creatinine in urine and ADMA in plasma and 0.5414 for nitrite in plasma. The AUC values for ADMA and nitrate were higher in the plasma compared to urine samples, whereas the AUC value for nitrite was lower in plasma compared to urine. In urine, the  $\delta$  (%) values (*y*) increased linearly with the average retention time (*x*) of the  $^{14}\text{N}/^{15}\text{N}$  isotopologs ( $y = -200 + 44 \times x$ ,  $r^2 = 1.000$ ,  $p < 0.0001$ ), indicating positive proportional error [5].

We tested for potential correlation between the AUC-ROC and Bland–Altman  $\delta$  (%) values. We found a strong correlation after Spearman between these approaches:  $r = 0.862$ ,  $p = 0.005$  (Figure 1A). This Figure also illustrates the AUC-ROC and  $\delta$  (%) differences for ADMA, nitrate and nitrite in the plasma and urine samples. Omitting the DMA values, a linear regression analysis between the AUC (*y*) and  $\delta$  (%) (*x*) values resulted in a straight line with the regression equation  $y = 0.59 + 2.38 \times x$ ,  $r^2 = 0.8673$  (Figure 1B).

In a further, recently performed study [17], we analyzed paired serum and urine samples of 85 volunteers who formerly had COVID-19 or were living with long-COVID-19. Nitrate, nitrite and creatinine were simultaneously analyzed by GC-MS on the apparatus ISQ and a 15 m long GC OPTIMA-17 column, as described previously [18]. The concentrations of the internal standards were 10 mM for creatinine in urine and 100  $\mu$ M in serum, 4  $\mu$ M for nitrite in serum and 8  $\mu$ M in urine as well as 40  $\mu$ M for nitrate in serum and 800  $\mu$ M in urine. Instead of toluene [13,14], ethyl acetate [21] was used for the extraction of the PFB derivatives, and 1  $\mu$ L aliquots of ethyl acetate extracts were injected in the splitless mode. The results of these analyses are summarized in Table 3.

The retention times of the corresponding isotopologs differed statistically significantly from each other. The values of IE,  $\delta$  and AUC differed for the isotopologs in urine and serum, as well as when compared to urine with serum. The highest IE,  $\delta$  and AUC values were observed for creatinine and the lowest were observed for nitrite in serum (Table 3). Figure 2 shows the relationship between the AUC-ROC and Bland–Altman values with respect to the retention times of the isotopologs in the serum and urine samples.

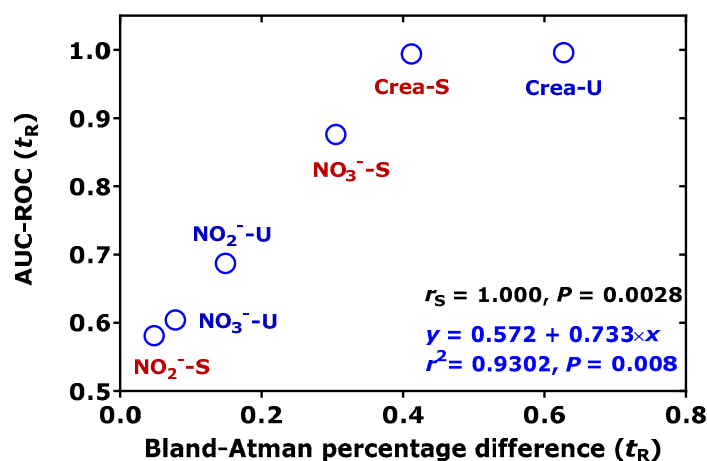


**Figure 2.** Comparison of the AUC-ROC values and the percentage difference values in the Bland–Altman approach with respect to the retention times in urine (U) and serum (S) samples of the isotopologs. There is a close correlation after Spearman between the two approaches and high linearity when the paired values for creatinine in urine are excluded.

### 3.2. Isotope Effects as a Measure of Matrix Effects in GC-MS: Proof-of-Concept Studies

Matrix effects are very common in LC-MS/MS, and methods have been proposed, with their measurements implemented in bioanalysis [22–26]. Matrix effects have been sporadically reported in GC-based methods, including GC-MS and GC-MS/MS [27–30]. Matrix-induced ion suppression effects occur both in electron ionization (EI) and NICI, yet the underlying mechanisms have not yet been explained thus far [26]. Stable-isotope-labeled analogs have been used in GC [31] and LC-MS/MS [32] to minimize matrix effects. To the best of our knowledge, isotopologs have not been used to quantify matrix effects in GC-MS or GC-MS/MS [26]. Given the observations of different IE and  $\delta$  values for some analytes in serum and urine samples in the present study, we tested the utility of isotopologs to quantify matrix effects in GC-MS.

**Table 3.** Summary of the results of the GC-MS (ISQ) analyses of the indicated analytes in paired samples in the present work obtained in urine (U) and serum (S) of 85 volunteers with long- or former COVID-19 infection. GC column, OPTIMA-17 (15 m × 0.25 mm I.D., 0.25 µm film thickness).

Analyte	Retention Time (min)	Wilcoxon Test ( $t_R$ )	IE	Wilcoxon Test (IE) (U vs. S)	$\delta$ (s)	Wilcoxon Test ( $\delta$ ) (U vs. S)	AUC ( $t_R$ )	AUC (IE) (U vs. S)	AUC ( $\delta$ ) (U vs. S)	Bland–Altman Percentage ( $t_R$ )	Bland–Altman Percentage (IE) (U vs. S)	Bland–Altman Percentage ( $\delta$ ) (U vs. S)
<sup>14</sup> N-Nitrate-U	3.183 (0.18)	$p < 0.0001$	1.0010 (0.14)	Nitrate $p < 0.0001$	0.1482 (176)	Nitrate $p < 0.0001$	0.6037 ± 0.0432 $p = 0.0196$	Nitrate $p < 0.0001$	Nitrate $p < 0.0001$	0.078 ± 0.136	Nitrate −0.228 ± 0.257	Nitrate −128 ± 126
<sup>15</sup> N-Nitrate-U	3.180 (0.18)		0.3025 (117)		0.6874 ± 0.0271 $p < 0.0001$							
<sup>14</sup> N-Nitrite-U	3.398 (0.20)	$p < 0.0001$	1.0010 (0.17)	Nitrite $p = 0.0036$	0.5859 (67)	Nitrite $p < 0.0001$	0.8756 ± 0.0432 $p < 0.0001$	Nitrite $p = 0.0077$	Nitrite $p = 0.0008$	0.305 ± 0.203	Nitrite 0.099 ± 0.200	Nitrite 99 ± 159
<sup>15</sup> N-Nitrite-U	3.393 (0.19)		0.0988 (245)		0.5814 ± 0.0434 $p = 0.652$							
<sup>14</sup> N-Nitrate-S	3.203 (0.16)	$p < 0.0001$	1.0030 (0.20)	Creatinine $p < 0.0001$	2.675 (18)	Creatinine $p < 0.0001$	0.9959 ± 0.0047 $p < 0.0001$	Creatinine $p < 0.0001$	Creatinine $p < 0.0001$	0.627 ± 0.114	Creatinine 0.217 ± 0.195	Creatinine 47 ± 51
<sup>15</sup> N-Nitrate-S	3.193 (0.03)		0.0988 (245)		0.9943 ± 0.0066 $p < 0.0001$							
<sup>14</sup> N-Nitrite-S	3.408 (0.13)	$p = 0.0005$	1.0000 (0.12)	Creatinine $p < 0.0001$	1.751 (41)	Creatinine $p < 0.0001$	0.9943 ± 0.0066 $p < 0.0001$	Creatinine $p < 0.0001$	Creatinine $p < 0.0001$	0.412 ± 0.167	Creatinine 0.217 ± 0.195	Creatinine 47 ± 51
<sup>15</sup> N-Nitrite-S	3.406 (0.15)		0.0988 (245)		0.9943 ± 0.0066 $p < 0.0001$							
<sup>1</sup> H-Creatinine-U	7.133 (0.07)	$p < 0.0001$	1.0060 (0.11)	Creatinine $p < 0.0001$	2.675 (18)	Creatinine $p < 0.0001$	0.9959 ± 0.0047 $p < 0.0001$	Creatinine $p < 0.0001$	Creatinine $p < 0.0001$	0.627 ± 0.114	Creatinine 0.217 ± 0.195	Creatinine 47 ± 51
<sup>2</sup> H <sub>3</sub> -Creatinine-U	7.089 (0.10)		0.0988 (245)		0.9943 ± 0.0066 $p < 0.0001$							
<sup>1</sup> H-Creatinine-S	7.130 (0.02)	$p < 0.0001$	1.0040 (0.17)	Creatinine $p < 0.0001$	1.751 (41)	Creatinine $p < 0.0001$	0.9943 ± 0.0066 $p < 0.0001$	Creatinine $p < 0.0001$	Creatinine $p < 0.0001$	0.412 ± 0.167	Creatinine 0.217 ± 0.195	Creatinine 47 ± 51
<sup>2</sup> H <sub>3</sub> -Creatinine-S	7.101 (0.17)		0.0988 (245)		0.9943 ± 0.0066 $p < 0.0001$							

### 3.2.1. GC-MS Analysis of Dimethyl Amine

We analyzed, via GC-MS,  $d_0$ -DMA and  $d_6$ -DMA after extractive derivatization with pentafluorobenzoyl chloride/toluene (Scheme 1) [16]. Human urine samples (U,  $n = 80$ ), a 67 mM potassium phosphate buffer of pH 7.0 (B,  $n = 33$ ), a 20 mM  $\text{Na}_2\text{CO}_3$  solution (C,  $n = 33$ ) and deionized water (W,  $n = 33$ ) were treated as follows:

- (1) A total of 10  $\mu\text{L}$  of a 1 mM  $d_6$ -DMA solution was introduced into autosampler glass vials;
- (2) A total of 10  $\mu\text{L}$  of U, B, C or W was added (B, C and W contained  $d_0$ -DMA at 0, 100 and 500  $\mu\text{M}$ );
- (3) A total of 90  $\mu\text{L}$  of W was added;
- (4) A total of 100  $\mu\text{L}$  of 20 mM  $\text{Na}_2\text{CO}_3$  was added.

$d_6$ -DMA was used as the internal standard at a fixed final concentration of 1000  $\mu\text{M}$  in all matrices. The  $d_0$ -DMA concentrations in B, C and W were 0, 100 and 500  $\mu\text{M}$ . After derivatization, 1  $\mu\text{L}$  aliquots of toluene extracts were injected splitless, and SIM of  $m/z$  240 for  $d_0$ -DMA and  $m/z$  246 for  $d_6$ -DMA was performed (ISQ apparatus, 15 m long OPTIMA-17 column). The results of this experiment are summarized in Table 4.

**Table 4.** Summary of the results of the GC-MS (ISQ) analyses of  $d_0$ -DMA in urine (U), buffer (B), carbonate (C) and deionized water (W) after extractive derivatization with pentafluorobenzoyl chloride and toluene. GC column: OPTIMA-17 (15 m  $\times$  0.25 mm I.D., 0.25  $\mu\text{m}$  film thickness).

Analyte, Matrix	Retention Time (min)	W or M-W Test ( $t_R$ )	IE	M-W Test (IE)	$\delta$ (s)	M-W Test ( $\delta$ )	Bland–Altman ( $\delta$ )	AUC ( $\delta$ )
$d_0$ -DMA-U	7.166 (0.12)	$p < 0.0001$	1.004 (0.06)		1.765 (16)			
$d_6$ -DMA-U	7.136 (0.16)							
$d_0$ -DMA-B	7.154 (0.07)	$p < 0.0001$	1.004 (0.04)	U vs. B 0.1863	1.690 (10)	U vs. B $p < 0.0001$	U vs. B 5.896 (15) % (−24–36)	U vs. B $0.7287 \pm 0.0594$ $p < 0.0001$
$d_6$ -DMA-B	7.125 (0.079)							
$d_0$ -DMA-C	7.155 (0.07)	$p < 0.0001$	1.004 (0.08)	U vs. C 0.3131	1.891 (18)	U vs. C $p = 0.2984$	U vs. C −4.076 (21) % (−45–36)	U vs. C $0.5577 \pm 0.0590$ $p = 0.3173$
$d_6$ -DMA-C	7.123 (0.07)							
$d_0$ -DMA-W	7.118 (0.06)	$p < 0.0001$	1.004 (0.04)	U vs. W 0.1413	1.715 (10)	U vs. W $p = 0.0017$	U vs. W 4.493 (14) % (−24–33)	U vs. W $0.6681 \pm 0.0621$ $p = 0.0036$
$d_6$ -DMA-W	7.090 (0.02)							

The PA of  $m/z$  246 for  $d_6$ -DMA-PFBz varied by 7.3%. In the urine samples ( $n = 80$ ), the PAR of  $m/z$  240 for  $d_0$ -DMA to  $m/z$  246 for  $d_6$ -DMA ranged between 0.1 and 1.6 (mean,  $0.608 \pm 0.26$ ).

The retention times of the isotopologs differed in all matrices but did not result in different IE values. This parameter was not further investigated. Statistically significant differences with respect to  $\delta$  were found between urine (U) and buffer (B), as well as between urine (U) and water (W) by the Mann–Whitney test and the ROC approach. The highest  $\delta$  value was observed for the carbonate solutions of DMA (C). The DMA solutions in B, C and W are more comparable among themselves than with the U samples, which were diluted 10-fold with water and carbonate. The experiment described above is a very simple simulation of potential matrix effects on isotope effects in GC-MS. A modification of this simulation, for instance, by using undiluted urine or urine diluted to varying degrees, would be more meaningful. Whether the Bland–Altman approach or the ROC approach

is able to provide more definite results remains to be investigated. The Bland–Altman approach is expected to be more promising because of its higher versatility.

### 3.2.2. GC-MS Analysis of Metformin

Standard curves were prepared for  $d_0$ -metformin ( $d_0$ -METF) in human urine (U) and serum (S) samples in relevant metformin concentration ranges, i.e., 0 to 25 mM in urine and 0 to 25  $\mu$ M in serum, using the internal standard at a fixed concentration of 1000  $\mu$ M for  $d_6$ -metformin ( $d_6$ -METF) in urine and 20  $\mu$ M in serum. SIM of  $m/z$  383 for  $d_0$ -METF and  $m/z$  383 for  $d_6$ -METF was performed as described previously [19]. The results of this experiment are summarized in Table 5. A typical GC-MS chromatogram from the analysis of metformin in a human serum sample is shown in Figure 3.

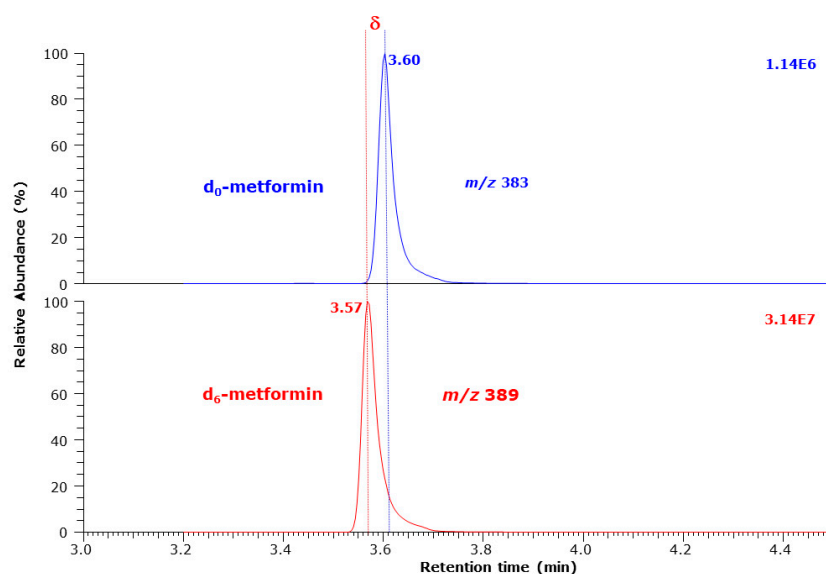


**Figure 3.** GC-MS chromatogram from the quantitative analysis of metformin in a human serum sample as pentafluoropropionyl (PFP) derivative on an ISQ instrument directly interfaced with a Trace 1310 series gas chromatograph. Selected ion monitoring of  $m/z$  383 for  $d_0$ -metformin and  $m/z$  389 for  $d_6$ -metformin (20  $\mu$ M) was performed (dwell time, 100 ms for each ion). Methane (2.4 mL/min) was used as the reagent gas for negative-ion chemical ionization. A fused-silica capillary column Optima 17 (15 m  $\times$  0.25 mm I.D., 0.25  $\mu$ m film thickness) was used. The oven temperature was kept at 40  $^{\circ}$ C for 0.5 min, then increased to 210  $^{\circ}$ C at a rate of 15  $^{\circ}$ C/min and to 320  $^{\circ}$ C at a rate of 35  $^{\circ}$ C/min, respectively, and held at 320  $^{\circ}$ C for 1 min. Helium was the carrier gas at a constant flow rate of 1 mL/min. The GC-MS method for metformin has been reported in detail elsewhere [19]. The symbol  $\delta$  indicates the difference between the retention times of  $d_0$ -metformin (3.60 min) and  $d_6$ -metformin (3.57 min).

The PA of  $m/z$  389 for  $d_6$ -METF-PFP varied by 31% in U and by 30% in S. The retention times of the isotopologs differed in both matrices. The IE and  $\delta$  values differed statistically significantly between U and S.

**Table 5.** Summary of the results of the GC-MS (ISQ) analyses of d<sub>0</sub>-metformin (d<sub>0</sub>-METF) and d<sub>6</sub>-metformin (d<sub>6</sub>-METF) in human urine (U) and serum (S) samples after derivatization with pentafluoropropionic anhydride in ethyl acetate. GC column: OPTIMA-17 (15 m × 0.25 mm I.D., 0.25 μm film thickness).

Analyte-Matrix	t <sub>R</sub> (min)	W Test (t <sub>R</sub> )	IE	M-W Test (IE)	δ(s)	M-W Test (δ)	t <sub>R</sub> Bland–Altman	t <sub>R</sub> ROC	IE U vs. S	δ U vs. S
d <sub>0</sub> -METF-U	3.628 (0.22)	p = 0.0002	1.014 (0.42)	U vs. S p < 0.0001	3.046 (30)	U vs. S p = 0.0003	U	U	Bland–Altman	Bland–Altman
d <sub>6</sub> -METF-U	3.589 (0.23)						1.409 (0.4157) % (0.59–2.22)	1.000 ± 0.000% (1 to 1) p < 0.0001	0.4889 (0.4291) % (−0.35–1.33)	39 (31) % (−23–101)
d <sub>0</sub> -METF-S	3.630 (0.00)	p = 0.0005	1.009 (0.11)	U vs. S p < 0.0001	1.90 (12)	U vs. S p = 0.0003	S	S	ROC	ROC
d <sub>6</sub> -METF-S	3.598 (0.11)						0.8762 ± 0.1083% (0.66–1.09)	1.000 ± 0.000% (1 to 1) p < 0.0001	0.9679 ± 0.0297 p < 0.0001	0.8846 ± 0.0709 p = 0.0011

#### 4. Discussion

The Bland–Altman approach has been proposed for testing agreement between two measurements [4]. The graphical Bland–Altman approach is frequently used in analytical chemistry to compare two analytical methods for the quantitative determination of analytes in biological samples [5]. The ROC approach is also a graphical plot that is often used to measure differences between two methods of measurement of analytes, although the main aim of this approach is testing disagreement between two approaches, especially in clinical diagnosis [33]. Given the potentially very small differences in the retention times of isotopologs in chromatography [1–3], we investigated, in the present study, the utility of the Bland–Altman and ROC approaches in the GC-MS analyses of selected endogenous analytes in human plasma, serum and urine samples. The focus of the study was on the main members of the L-arginine/nitric oxide pathway [11] and creatinine, which is an important clinical biochemical parameter.

Nitrate and nitrite and the externally added  $^{15}\text{N}$  isotopologs were analyzed by GC-MS after derivatization with PFB bromide to their PFB-ONO<sub>2</sub> and PFB-NO<sub>2</sub> derivatives, respectively (Scheme 1). PFB-ONO<sub>2</sub> and PFB-NO<sub>2</sub> are separated completely by GC as well as by MS. Being a nitric acid ester, PFB-ONO<sub>2</sub> eluted in front of PFB-NO<sub>2</sub>, which is a nitro derivative [13]. Virtually, both the Bland–Altman and the ROC approach are not able to discriminate  $^{14}\text{N}/^{15}\text{N}$  isotopologs of PFB-ONO<sub>2</sub> and PFB-NO<sub>2</sub>, respectively. Yet, small differences were detected in plasma, serum and urine samples, independent of the extraction solvent that contained the derivatives, i.e., toluene and ethyl acetate. In contrast, both the Bland–Altman approach and the ROC approach clearly discriminated the respective H/D isotopologs of DMA (PFBz-DMA), ADMA (Me-PFP), Arg (Me-PFP) and creatinine (PFB-creatinine) (Scheme 1), yet with some differences for ADMA between plasma and urine. The strong correlation found between the Bland–Altman and the ROC approaches suggests that both methods are virtually equally suitable to investigate isotope effects in GC-MS.

The two methyl groups of DMA in its PFBz derivative, the methyl group of creatinine in its PFB derivative and the methyl ester groups of Arg and ADMA in the methyl ester PFP derivatives are most likely responsible for the considerably stronger H/D isotope effects compared to the  $^{14}\text{N}/^{15}\text{N}$  isotope effects observed in PFB-ONO<sub>2</sub> and PFB-NO<sub>2</sub> derivatives. The greater differences in physical properties between H and D (a 100% increase in mass) compared to the differences between  $^{14}\text{N}$  and  $^{15}\text{N}$  (a 7% increase in mass) are a likely explanation for the stronger H/D isotope effects.

The charge radius of D is 2.5 times higher compared to the charge radius of H (<https://physics.nist.gov/cuu/Constants/index.html>, assessed on 10 December 2023). The gravest factor that causes the stronger H/D isotope effects is likely to be a stronger interaction of the methyl groups with the lipophilic stationary phase of the GC column (50% methylpolysiloxane, 50% phenylpolysiloxane) in the present study. H/D effects were observed for non-derivatized methylxanthine isotopologs in GC-MS on a 14% cyanopropylphenyl methylpolysiloxane fused silica column [34]. In that study, H/D isotopic effects were found to depend not only on the number of D atoms but also on the position of the CD<sub>3</sub> groups in the molecules (IE range, 1.00147 to 1.00668) [34]. The rate of a reaction involving a C–H bond is typically 6–10 times faster than the corresponding C–D bond [35].

In the case of PFB-ONO<sub>2</sub> and PFB-NO<sub>2</sub>, the central N atoms seem to be strongly sterically hindered from interacting with the stationary phase. The differences seen between PFB-ONO<sub>2</sub> and PFB-NO<sub>2</sub> suggest that the N atom in PFB-ONO<sub>2</sub> is somewhat more accessible to interaction with the stationary phase than the N atom in PFB-NO<sub>2</sub>, which is closer to the PFB group (Scheme 1). This observation demands deeper investigations with nitro and nitric acid derivatives of alkyl/aryl residues.

In the cases of ADMA, nitrate, nitrite and creatinine, which were analyzed both in plasma/serum and in urine, there were some differences in the Bland–Altman  $\delta$  (%) and ROC-AUC values in plasma or serum compared to urine. ADMA: 0.1409 vs. 0.1298 (1.1-fold); nitrate: 0.06909 vs. 0.04029 (1.7-fold); nitrite: 0.00841 vs. 0.02891 (0.3-fold). These

observations may be interpreted as a type of “matrix effect”. Matrix effects occur not only in LC-MS/MS but also in GC-MS and GC-MS/MS [22–32]. Several methods have been proposed and used in LC-MS/MS, such as the use of standard line slopes as a measure of relative matrix effects [22]. The results of the present study, including those of the pilot experiment, indicate that the differences in the retention times of isotopologs  $\delta$  are better suited to quantify matrix effects than the ratio of the retention times IE of  $d_0$ -DMA-PFBz and  $d_6$ -DMA-PFBz in human urine. IE is a little variable measure but is less sensitive than the more variable measure  $\delta$ . The Bland–Altman approach seems to be better suited for quantitating isotope effects than the ROC approach.

## 5. Conclusions

In GC-MS, the Bland–Altman and ROC approaches seem to be suitable for studying H/D and  $^{14}\text{N}/^{15}\text{N}$  isotope effects in the PFB, PFBz and PFP derivatives of endogenous analytes of the L-arginine/nitric oxide pathway and the universal biomarker creatinine. Isotope effects in GC-MS are likely to be caused by differences in the interaction strengths of H/D and  $^{14}\text{N}/^{15}\text{N}$  isotopes in the derivatives with the hydrophobic stationary phase of the GC column. D atoms in the derivatives seem to attenuate the interaction of the skeleton of the molecules with the lipophilic GC stationary phase. Differences in the retention times of isotopologs, i.e., the parameter  $\delta$ , appear to be a better-suited experimental measure for quantitating matrix effects in GC-MS.

**Funding:** This research received no external funding.

**Institutional Review Board Statement:** In this study, material from previously approved human studies was used (see Section 2.1).

**Informed Consent Statement:** Not applicable (see Section 2.1).

**Data Availability Statement:** The data presented in this study are available in article.

**Acknowledgments:** The author is grateful to previous and current members of his group for their contributions.

**Conflicts of Interest:** The author declares no conflict of interest.

## References

1. Biemann, K. *Mass Spectrometry—Organic Chemical Applications*; McGraw Hill: New York, NY, USA, 1962; p. 204.
2. Lehmann, W.D. A timeline of stable isotopes and mass spectrometry in the life sciences. *Mass Spectrom. Rev.* **2017**, *36*, 58–85. [[CrossRef](#)]
3. Turowski, M.; Yamakawa, N.; Meller, J.; Kimata, K.; Ikegami, T.; Hosoya, K.; Tanaka, N.; Thornton, E.R. Deuterium isotope effects on hydrophobic interactions: The importance of dispersion interactions in the hydrophobic phase. *J. Am. Chem. Soc.* **2003**, *125*, 13836–13849. [[CrossRef](#)]
4. Bland, J.M.; Altman, D.G. Statistical methods for assessing agreement between two methods of clinical measurement. *Lancet* **1986**, *1*, 307–310. [[CrossRef](#)]
5. Tsikas, D. Mass Spectrometry-Based Evaluation of the Bland-Altman Approach: Review, Discussion, and Proposal. *Molecules* **2023**, *28*, 4905. [[CrossRef](#)]
6. Gucciardi, A.; Cogo, P.E.; Traldi, U.; Eaton, S.; Darch, T.; Simonato, M.; Ori, C.; Carnielli, V.P. Simplified method for microlitre deuterium measurements in water and urine by gas chromatography-high-temperature conversion-isotope ratio mass spectrometry. *Rapid Commun. Mass Spectrom.* **2008**, *22*, 2097–2103. [[CrossRef](#)]
7. Wong, W.W.; Roberts, S.B.; Racette, S.B.; Das, S.K.; Redman, L.M.; Rochon, J.; Bhaskar, M.V.; Clarke, L.L.; Kraus, W.E. The doubly labeled water method produces highly reproducible longitudinal results in nutrition studies. *J. Nutr.* **2014**, *144*, 777–783. [[CrossRef](#)]
8. Wong, W.W.; Clarke, L.L. Accuracy of  $\delta(18)\text{O}$  isotope ratio measurements on the same sample by continuous-flow isotope-ratio mass spectrometry. *Rapid Commun. Mass Spectrom.* **2015**, *29*, 2252–2256. [[CrossRef](#)]
9. Zweig, M.H.; Campbell, G. Receiver-operating characteristic (ROC) plots: A fundamental evaluation tool in clinical medicine. *Clin. Chem.* **1993**, *39*, 561–577. [[CrossRef](#)]
10. Tom, F. An Introduction to ROC Analysis. *Pattern Recognit. Lett.* **2006**, *27*, 861–874. [[CrossRef](#)]
11. Tsikas, D. A critical review and discussion of analytical methods in the L-arginine/nitric oxide area of basic and clinical research. *Anal. Biochem.* **2008**, *379*, 139–163. [[CrossRef](#)]

12. Tsikas, D. Urinary Dimethylamine (DMA) and Its Precursor Asymmetric Dimethylarginine (ADMA) in Clinical Medicine, in the Context of Nitric Oxide (NO) and Beyond. *J. Clin. Med.* **2020**, *9*, 1843. [[CrossRef](#)]
13. Tsikas, D. Simultaneous derivatization and quantification of the nitric oxide metabolites nitrite and nitrate in biological fluids by gas chromatography/mass spectrometry. *Anal. Chem.* **2000**, *72*, 4064–4072. [[CrossRef](#)]
14. Tsikas, D.; Wolf, A.; Mitschke, A.; Gutzki, F.M.; Will, W.; Bader, M. GC-MS determination of creatinine in human biological fluids as pentafluorobenzyl derivative in clinical studies and biomonitoring: Inter-laboratory comparison in urine with Jaffé, HPLC and enzymatic assays. *J. Chromatogr. B* **2010**, *878*, 2582–2592. [[CrossRef](#)]
15. Tsikas, D.; Schubert, B.; Gutzki, F.M.; Sandmann, J.; Frölich, J.C. Quantitative determination of circulating and urinary asymmetric dimethylarginine (ADMA) in humans by gas chromatography-tandem mass spectrometry as methyl ester tri(N-pentafluoropropionyl) derivative. *J. Chromatogr. B* **2003**, *798*, 87–99. [[CrossRef](#)]
16. Tsikas, D.; Thum, T.; Becker, T.; Pham, V.V.; Chobanyan, K.; Mitschke, A.; Beckmann, B.; Gutzki, F.M.; Bauersachs, J.; Stichtenoth, D.O. Accurate quantification of dimethylamine (DMA) in human urine by gas chromatography-mass spectrometry as pentafluorobenzamide derivative: Evaluation of the relationship between DMA and its precursor asymmetric dimethylarginine (ADMA) in health and disease. *J. Chromatogr. B* **2007**, *851*, 229–239. [[CrossRef](#)]
17. Mikuteit, M.; Baskal, B.; Klawitter, S.; Dopfer-Jablonka, A.; Behrens, G.M.N.; Müller, F.; Schröder, D.; Klawonn, F.; Steffens, S.; Tsikas, D. Amino acids, post-translational modifications, nitric oxide, and oxidative stress in serum and urine of long COVID and ex COVID human subjects. *Amino Acids* **2023**, *55*, 1173–1188. [[CrossRef](#)]
18. Bollenbach, A.; Schutte, A.E.; Kruger, R.; Tsikas, D. An Ethnic Comparison of Arginine Dimethylation and Cardiometabolic Factors in Healthy Black and White Youth: The ASOS and African-PREDICT Studies. *J. Clin. Med.* **2020**, *9*, 844. [[CrossRef](#)]
19. Baskal, S.; Bollenbach, A.; Henzi, B.; Hafner, P.; Fischer, D.; Tsikas, D. Stable-Isotope Dilution GC-MS Measurement of Metformin in Human Serum and Urine after Derivatization with Pentafluoropropionic Anhydride and Its Application in Becker Muscular Dystrophy Patients Administered with Metformin, L-Citrulline, or Their Combination. *Molecules* **2022**, *27*, 3850. [[CrossRef](#)]
20. Carlson, R.V.; Boyd, K.M.; Webb, D.J. The revision of the Declaration of Helsinki: Past, present and future. *Br. J. Clin. Pharmacol.* **2004**, *57*, 695–713. [[CrossRef](#)]
21. Hanff, E.; Eisenga, M.F.; Beckmann, B.; Bakker, S.J.L.; Tsikas, D. Simultaneous Pentafluorobenzyl Derivatization and GC-ECNICAL-MS Measurement of Nitrite and Malondialdehyde in Human Urine: Close Positive Correlation between These Disparate Oxidative Stress Biomarkers. *J. Chromatogr. B* **2017**, *1043*, 167–175. [[CrossRef](#)]
22. Matuszewski, B.K.; Constanzer, M.L.; Chavez-Eng, C.M. Matrix effect in quantitative LC/MS/MS analyses of biological fluids: A method for determination of finasteride in human plasma at picogram per milliliter concentrations. *Anal. Chem.* **1998**, *70*, 882–889. [[CrossRef](#)]
23. Matuszewski, B.K.; Constanzer, M.L.; Chavez-Eng, C.M. Strategies for the assessment of matrix effect in quantitative bioanalytical methods based on HPLC-MS/MS. *Anal. Chem.* **2003**, *75*, 3019–3030. [[CrossRef](#)]
24. Matuszewski, B.K. Standard line slopes as a measure of a relative matrix effect in quantitative HPLC-MS bioanalysis. *J. Chromatogr. B* **2006**, *830*, 293–300. [[CrossRef](#)]
25. Cortese, M.; Gigliobianco, M.R.; Magnoni, F.; Censi, R.; Di Martino, P.D. Compensate for or Minimize Matrix Effects? Strategies for Overcoming Matrix Effects in Liquid Chromatography-Mass Spectrometry Technique: A Tutorial Review. *Molecules* **2020**, *25*, 3047. [[CrossRef](#)]
26. Panuwet, P.; Hunter, R.E., Jr.; D'Souza, P.E.; Chen, X.; Radford, S.A.; Cohen, J.R.; Marder, M.E.; Kartavenka, K.; Ryan, P.B.; Barr, D.B. Biological Matrix Effects in Quantitative Tandem Mass Spectrometry-Based Analytical Methods: Advancing Biomonitoring. *Crit. Rev. Anal. Chem.* **2016**, *46*, 93–105. [[CrossRef](#)]
27. Erney, D.R.; Gillespie, A.M.; Gilvydis, D.M.; Poole, C.F. Explanation of the Matrix-Induced Chromatographic Response Enhancement of Organophosphorus Pesticides during Open-Tubular Column Gas-Chromatography with Splitless or Hot on-Column Injection and Flame Photometric Detection. *J. Chromatogr. A* **1993**, *638*, 57–63. [[CrossRef](#)]
28. Schenck, F.J.; Lehotay, S.J. Does further clean-up reduce the matrix enhancement effect in gas chromatographic analysis of pesticide residues in food? *J. Chromatogr. A* **2000**, *868*, 51–61. [[CrossRef](#)]
29. Hajslova, J.; Zrostlikova, J. Matrix effects in (ultra)trace analysis of pesticide residues in food and biotic matrices. *J. Chromatogr. A* **2003**, *1000*, 181–197. [[CrossRef](#)]
30. Yu, S.; Xu, X.M. Study of matrix-induced effects in multi-residue determination of pesticides by online gel permeation chromatography-gas chromatography/mass spectrometry. *Rapid Commun. Mass Spectrom.* **2012**, *26*, 963–977. [[CrossRef](#)]
31. Colby, B.N.; McCaman, M.W. A comparison of calculation procedures for isotope dilution determinations using gas chromatography mass spectrometry. *Biomed. Mass Spectrom.* **1979**, *6*, 225–230. [[CrossRef](#)]
32. Berg, T.; Strand, D.H. C-13 labelled internal standards-A solution to minimize ion suppression effects in liquid chromatography-tandem mass spectrometry analyses of drugs in biological samples? *J. Chromatogr. A* **2011**, *1218*, 9366–9374. [[CrossRef](#)] [[PubMed](#)]
33. Datta, K.; LaRue, R.; Permpalung, N.; Das, S.; Zhang, S.; Steinke, M.; Bushkin, Y.; Nosanchuk, J.D.; Marr, K.A. Development of an Interferon-Gamma Release Assay (IGRA) to Aid Diagnosis of Histoplasmosis. *J. Clin. Microbiol.* **2022**, *60*, e0112822. [[CrossRef](#)] [[PubMed](#)]

34. Benchekroun, Y.; Dautraix, S.; Désage, M.; Brazier, J.L. Isotopic effects on retention times of caffeine and its metabolites 1,3,7-trimethyluric acid, theophylline, theobromine and paraxanthine. *J. Chromatogr. B* **1997**, *688*, 245–254. [[CrossRef](#)] [[PubMed](#)]
35. Laidler, K.J. *Chemical Kinetics*, 3rd ed.; Harper & Row: New York, NY, USA, 1987; ISBN 978-0-06-043862-3.

**Disclaimer/Publisher's Note:** The statements, opinions and data contained in all publications are solely those of the individual author(s) and contributor(s) and not of MDPI and/or the editor(s). MDPI and/or the editor(s) disclaim responsibility for any injury to people or property resulting from any ideas, methods, instructions or products referred to in the content.